



LAWRENCE
LIVERMORE
NATIONAL
LABORATORY

Multiple Beam Induction Accelerators for Heavy Ion Fusion

P. A. Seidl, J. J. Barnard, A. Faltens, A. Friedman,
W. L. Waldron

October 17, 2013

Nuclear Instruments and Methods A

Disclaimer

This document was prepared as an account of work sponsored by an agency of the United States government. Neither the United States government nor Lawrence Livermore National Security, LLC, nor any of their employees makes any warranty, expressed or implied, or assumes any legal liability or responsibility for the accuracy, completeness, or usefulness of any information, apparatus, product, or process disclosed, or represents that its use would not infringe privately owned rights. Reference herein to any specific commercial product, process, or service by trade name, trademark, manufacturer, or otherwise does not necessarily constitute or imply its endorsement, recommendation, or favoring by the United States government or Lawrence Livermore National Security, LLC. The views and opinions of authors expressed herein do not necessarily state or reflect those of the United States government or Lawrence Livermore National Security, LLC, and shall not be used for advertising or product endorsement purposes.

Multiple beam induction accelerators for heavy ion fusion

Peter A. Seidl^a, John J. Barnard^b, Andris Faltens^a, Alex Friedman^b, William L. Waldron^a

^a*Lawrence Berkeley National Laboratory*

^b*Lawrence Livermore National Laboratory*

Submitted October 8, 2012

Revised February 23, 2013

Abstract: Induction accelerators are appealing for heavy-ion driven inertial fusion energy (HIF) because of their high efficiency and their demonstrated capability to accelerate high beam current (≥ 10 kA in some applications). For the HIF application, accomplishments and challenges are summarized. HIF research and development has demonstrated the production of single ion beams with the required emittance, current, and energy suitable for injection into an induction linear accelerator. Driver scale beams have been transported in quadrupole channels of the order of 10% of the number of quadrupoles of a driver. We review the design and operation of induction accelerators and the relevant aspects of their use as drivers for HIF. We describe intermediate research steps that would provide the basis for a heavy-ion research facility capable of heating matter to fusion relevant temperatures and densities, and also to test and demonstrate an accelerator architecture that scales well to a fusion power plant.

1 **1 Motivation**

2 The three main types of heavy ion drivers for inertial fusion energy are synchrotrons, RF
3 linear accelerators (usually with storage rings) and induction linear accelerators. RF
4 accelerators are appealing because of the extensive experience in high energy and nuclear
5 physics; induction accelerators, because of their higher efficiency and experience
6 accelerating high beam current (≥ 10 kA in some applications). The US effort has focused
7 on induction accelerators because of the high efficiency at high beam current and because
8 there is no need to accumulate charge in storage rings; their non-resonant character
9 allows pulse compression during acceleration. Baseline driver design in the US consists
10 of a multiple beam induction linear accelerator, accelerating beams to a final kinetic
11 energy of 1 GeV per ion, or higher. Because of the high charge per bunch, transport, or
12 transverse control of the beam, is the limiting consideration at low ion kinetic energy.
13 The approach is to accelerate a longer bunch near the transport limit and gradually
14 decrease its length within the accelerator -- as allowed by beam dynamics -- by small
15 voltage ramps. The transport limit for current increases with velocity because of the
16 increasing strength of the $\mathbf{v} \times \mathbf{B}$ force. Near the exit of the accelerator, a larger ramp is
17 applied to compress the bunch. This final bunch compression occurs mainly at the end of
18 the accelerator and in the drift lines leading to the target, resulting in the required short
19 pulse at the target.

20 To put the driver objectives and components in context, Fig. 1 shows a typical layout of a
21 multi-beam induction linear accelerator driver for heavy ion fusion. Operating at 5-15 Hz,
22 many ion beams are injected into an induction accelerator, with the bundle of beams
23 passing through common induction accelerator cores. Other induction accelerator
24 architectures have been studied, for example, separate accelerators for each beamline, and
25 recirculating induction accelerators. Initially motivated by their potential to lower cost,
26 studies showed additional beam physics and technical issues, as described in Ref.
27 [Ta11], chapter 10.

28 Singly charged ($q = 1$) ions are often chosen because higher charge state ions create
29 proportionally more space charge which would be much more difficult to produce and
30 match to the alternating gradient lattice. Other favorable aspects of $q=1$ ions are the

ability to create low-emittance beams of sufficiently high current with essentially no admixture of $q \geq 2$ ions, and the lower longitudinal confinement fields required for bunch containment. Of course, a disadvantage is the proportionally lower acceleration rate. Ion sources and injectors for HIF are reviewed by Kwan [Kw05]. The accelerator front end may use electrostatic focusing quadrupoles at the front end, followed by a transition to superconducting magnetic quadrupoles for most ($> 90\%$) of the accelerator.

A velocity ramp is applied to the beam near the end of the accelerator. The beam ($\beta = 0.2 - 0.3$) is not highly relativistic, thus the bunch length shortens by an order of magnitude or more to meet the 1-10 ns bunch duration required by the target. This drift-compression section and the final focusing system are reviewed by Kaganovich et al. [Ka12] in these proceedings. A part of the drift compression section includes dipoles for each beamline to aim each beam at the target according to the required illumination geometry.

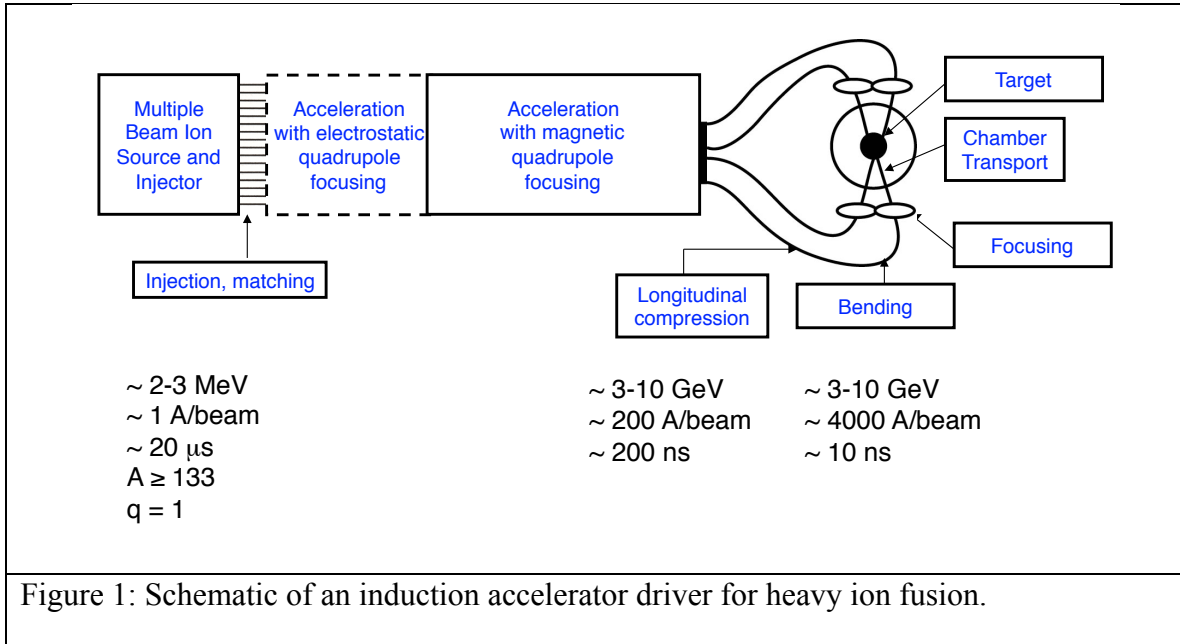
The propagation of the beams in the reactor chamber is reviewed by Olson [Ol12]. The ends of each beamline must penetrate the reactor chamber wall while leaving sufficient solid angle for a viable tritium breeding blanket and heat extraction. This blanket design is usually a flowing thick layer of liquid, molten salt containing lithium, which protects the structural wall and focusing magnet coils from radiation damage [Mo12]. This is a very desirable feature that is compatible with ion-beam driven IFE. Not shown in Fig. 1 are the essential tritium extraction, target factory, heat recovery and electricity generation systems.

Fundamental aspects of the fusion target designs (ignition mode, target size, energy coupling) have a great influence on the final beam parameters and target illumination geometry [Ba12] and therefore on the accelerator design. The required beam energy per pulse may vary among target designs by a factor of several, which will influence the number of parallel beams and other aspects of the accelerator design. Also, the beam pulse duration depends on the ignition mode, with “fast-ignition” targets requiring sub-nanosecond ignition pulses, and indirectly driven targets requiring ~ 10 ns main pulses. Most targets generally require a low power prepulse, with 20 - 100 ns duration to efficiently compress the fusion fuel prior to the main pulse. Since the driver is considered

to be the most costly aspect of the IFE system, the target design has a tremendous impact on the system cost and feasibility. In this paper, we assume final beam parameters of approximately $5 \pm 2 \text{ MJ/pulse}$ (total of the foot and the main pulse), $5 \pm 3 \text{ GeV}$ ion kinetic energy, and an ignition pulse of $10 \pm 5 \text{ ns}$ and a final beam radius at the target of $5 \pm 3 \text{ mm}$. These values correspond to a variety of indirectly driven hohlraum target designs. At the end of the accelerator the overall bunch duration is assumed to be $0.1 - 0.2 \text{ }\mu\text{s}$. Hypothetically, if considerably greater beam energy ($> 7 \text{ MJ/pulse}$) were required for ignition and satisfactory target gain, the capital costs significantly increase even though the cost of electricity scales favorably for higher yield targets requiring higher energy driver pulses.

As will be described below, these beam parameters are at once somewhat conservative in their demands on the accelerator, but still require the development of novel accelerator components, and the understanding and mitigation of various beam physics that can dilute the beam emittance. Target designs requiring a much shorter ignition pulse ($< 1 \text{ ns}$), or a smaller radius at the target ($< 1 \text{ mm}$) usually force a higher beam phase space density at the target, corresponding to stricter tolerances throughout the accelerator. Lee reviews beam dynamics in induction accelerators for HIF in these proceedings [Le12].

The trade-offs between target physics and accelerator physics must be resolved with an overall HIF design optimization. For example, to simplify some target design challenges, a few driver designs have two ion kinetic energy beams striking the target for different parts of the pulse [Yu03]. This invokes additional accelerator design challenges – to separate a group of beams for further acceleration, implementation of needed delay lines [Fr12], and the necessity to determine the economic costs of these features.



Common to laser and ion beam IFE development plans is a demonstration power plant (DEMO) that should produce fusion power, breed tritium and demonstrate all key scientific and engineering points [Na13]. To develop the science and technology for HIF, several intermediate step induction accelerators have been suggested or built. These may be categorized by low (< 100 J/pulse) and high (10 - 100 kJ) energy per pulse. The purpose of the low energy (< 100 J) experiments, included developing and testing injection and transport of a high space-charge beam while preserving the low emittance that would be needed for ultimate focusing onto a small fusion target. While the kinetic energy and beam current in some of these experiments was often much lower than needed at any stage of a driver, the transport lattices were designed so that the dimensionless perveance and betatron phase advance matched those in a driver. Thus the relative importance of space charge to emittance mimicked a driver. An example is the Single Beam Transport Experiment [Ti85] that demonstrated space-charge dominated transport through 87 electrostatic quadrupoles with very little emittance growth. In other experiments, for example the 2-MV injector experiment [Bi05] and the High Current Experiment [Pr05], the beam current (0.2 - 0.7 A) and energy (1 - 2 MeV) were characteristic of an injected ion beam to the low energy end of an induction linac. These experiments demonstrated the needed low emittance from the source and injector at driver scale, as well as the ability to control the high initial space charge and match the

beam to an alternating gradient quadrupole lattice. Other experiments are summarized in a review article by Sharp et al. [Sh11]. The objective of the proposed 10 - 100 kJ accelerator and research facility is to definitively demonstrate all the key driver beam manipulations at or near full scale, and to enable HIF relevant target physics experiments. It is usually considered a prerequisite to the DEMO. For example, in the late 1970's the Heavy Ion Demonstration Experiment proposal was for a 50 - 100 kJ/pulse facility for which RF and induction accelerator designs were developed [Go79]. The more recent proposals are the Integrated Research Experiment (IRE) [Ba01] and the Heavy Ion Driver Implosion Experiment (HIDIX) [Lo11], both based on multiple-beam induction linear accelerator with quadrupole focusing to create 10 - 100-kJ beam bunches.

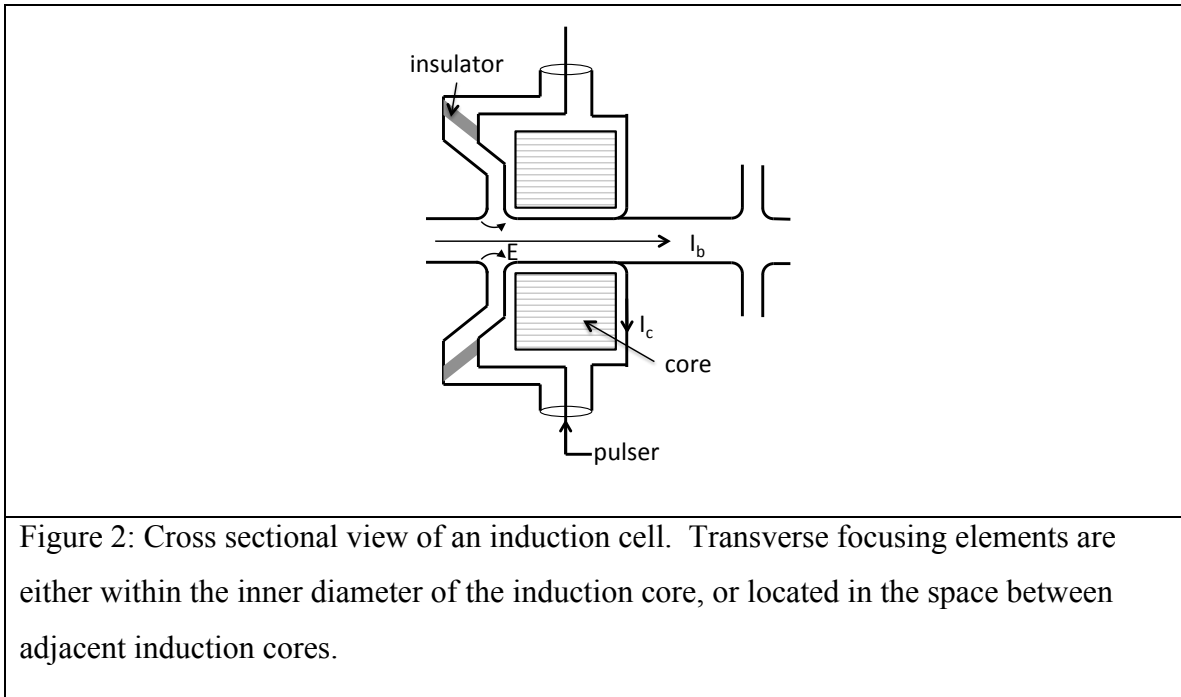
2 Induction linear accelerators

An induction linear accelerator is a non-resonant (low-Q) structure in which the acceleration field is established by a high voltage pulse across the gap. The induction core presents a high impedance to prevent the pulser from seeing a short circuit (Fig. 2). The gap geometry establishes the accelerating electric field along the beamline. The field distribution is analogous to a sequence of DC voltage gaps, with the difference that the voltage along the beamline is not cumulative. If the magnetization current in the core is low, and the beam current is high, the acceleration of the beam ions can have very high electrical efficiency. The development and first implementation of induction linacs was for the electron beam in the ASTRON magnetic confinement fusion experiment [Ch58]. Since then, many induction linear accelerators have been built in the US, Japan, France, Russia and China for applications such as x-ray FELs, flash radiography, the simulation of weapons effects and inertial fusion. Except for the inertial fusion application, most instances are electron linacs. Reference [Ta11] is a helpful review of the principles and applications of induction accelerators.

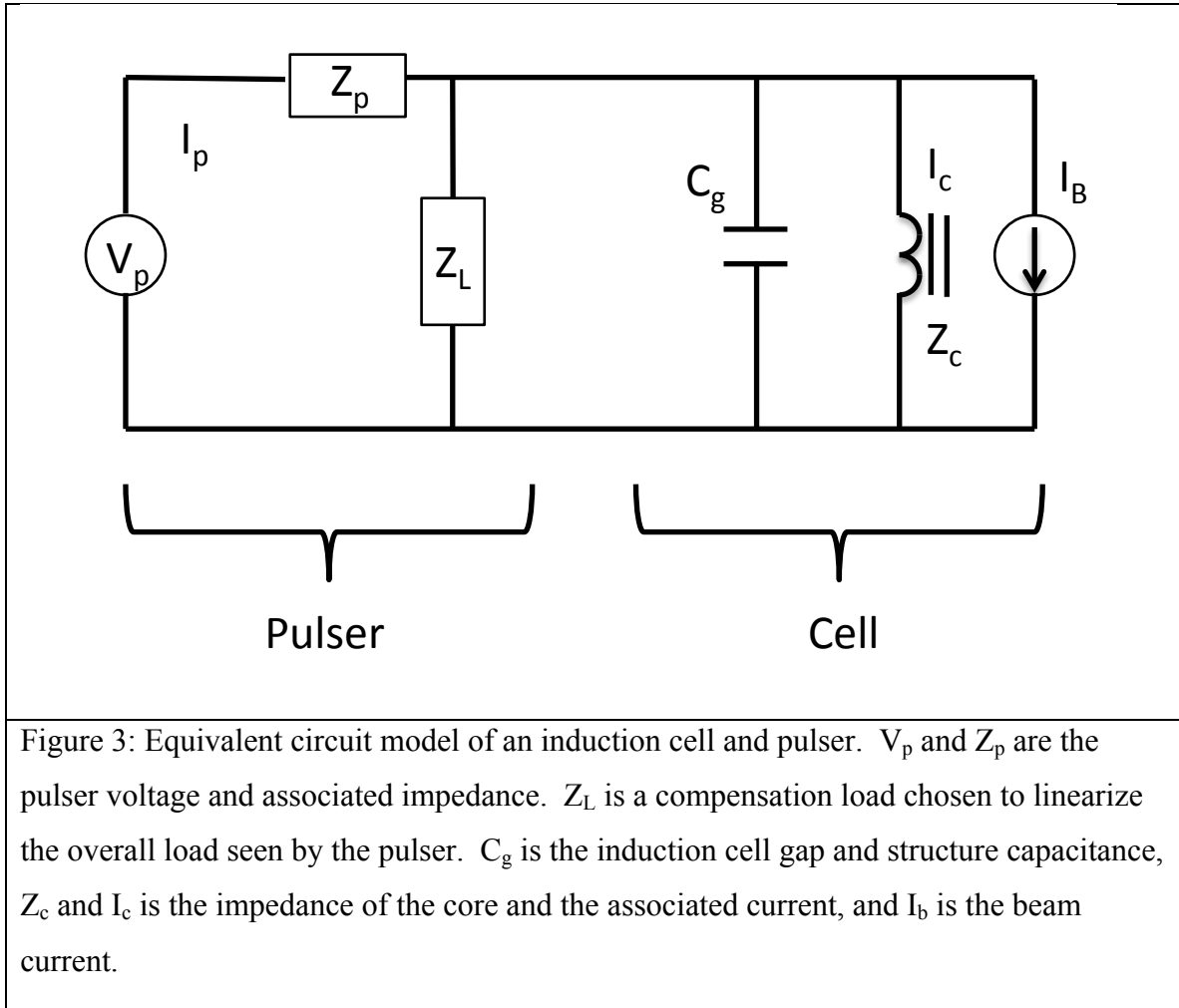
In Fig. 2, the beam focusing elements are inside r_i , the inner radius of the induction core. The voltage across the accelerating gap and the voltage pulse duration are related to the magnetic flux swing in the core material and the cross sectional area via Faraday's law of induction. The relationship is often simplified to:

132
$$\Delta B \cdot A = \Delta V \cdot \Delta t \quad (\text{Eq. 1})$$

133 The voltage must also be sustained across the insulator, which is a critical design
 134 component and is often angled and out of the line of sight of the acceleration gap and the
 135 beam to minimize the probability of initiating an electrical breakdown. Since the drive
 136 current pulse is significant, the induction cores may be driven from multiple coaxial drive
 137 lines around the circumference to symmetrize the stray fields from the current pulses that
 138 would steer the beam transversely. This is more of a concern for induction modules for
 139 acceleration of electrons (vs ions) due to the lower rigidity of the electrons. The cross
 140 sectional area per meter of the toroidal induction core is proportional to the difference in
 141 of the outer and inner radius, $(r_o - r_i)$, while the mass of the induction core is
 142 proportional to $(r_o^2 - r_i^2)$. Due to the cost of the induction core material, there is an
 143 economic incentive to keep the inner radius small.



144
 145 Figure 3 shows a lumped circuit model of the induction acceleration cell and pulser. The
 146 efficiency, as measured by the ratio of I_b to I_p is greatest for high beam current. Typical
 147 drive currents for an induction core are on the order of a kiloampere, thus similarly high
 148 beam currents can result in electrical efficiency of 50% or higher.



149

150 High efficiency has been demonstrated in various electron induction accelerators, and
 151 some examples are given in Table 1. Including other power consumption, estimates of
 152 total accelerator efficiency in existing accelerators (for which efficiency has not been a
 153 major concern) tend to be much lower because of the power consumed by room
 154 temperature magnets, vacuum pumps, and other components. However, a noteworthy
 155 example is Astron, which could generate 300 ns pulses at 60 Hz (but more typically ran
 156 at ≈ 5 Hz), with an average beam power of 86 kW. Because the project goals did not
 157 require higher efficiency, the overall wall-plug efficiency was greatly impacted by the
 158 power requirements of the room-temperature focusing solenoids, and aspects of the
 159 pulsed power technology. Nevertheless, the overall efficiency was still $\approx 10\%$, a notable
 160 accomplishment at the time.

For a heavy-ion driver using superconducting focusing magnets and modern pulsed-power technology operating at ≥ 5 Hz, the core loss (eddy current losses in the laminations of the magnetic material) in induction acceleration modules is the most important factor in overall wall-plug efficiency. Within the HIF acceleration modules, additional contributions to driver efficiency are the pulser efficiency ($\approx 85\%$) and energy expended in the acceleration waveforms before and after the passage of the pulse (waveform rise time and fall time). Average losses of 1 W/lattice period in the magnet leads of each array module, and 1 W/m² within the superconducting magnets beam tubes result in relatively little power required of the focusing magnet refrigeration system.

Accelerator	Drive current (kA)	Beam current (kA)	Repetition Rate (Hz)	Efficiency (%)
Astron	2	0.8	60	40
ATA	20	10	5	50
ETA II	5	3	2	60
DARHT II	10	2	<1	20

Table 1: Accelerator core efficiency, expressed as the ratio of beam current to drive current, for several high-current induction accelerators. Many other examples of induction accelerators are summarized in Ref. [Ta11].

2.1 Pulsers

An IFE power plant operating at ≈ 10 Hz would generate 3×10^8 pulses per year and perhaps 10^{10} pulses over the lifetime of the driver. This is the motivation for developing long lifetime components.

The beam pulse specifications determine the pulser voltage and accuracy requirements. At the low energy end of the driver, the pulse duration starts at > 10 μ s, but is compressed to < 1 μ s as quickly as the beam dynamics allow. The compression amplifies the beam current and in turn increases the electrical efficiency and reduces the core volume. For most of the accelerator, the pulse duration is $t_p \approx 0.2$ μ s with a relatively short rise and fall time (≤ 0.05 μ s). At 1 mC/bunch distributed over many beams, the total current in the pulse is ≈ 5 kA. This leads to an attractively efficient accelerator.

Note that these values are approximate. The pulse width, and associated rise and fall times could be longer or shorter depending on the capabilities of the modulator and economics. Waveforms, or the average of a group of waveforms in adjacent cells must be flat to a high degree ($\sim 1\%$). Random errors are partly suppressed due to statistical averaging with many other cells (See Section 3).

The beam bunch, including its own rise and fall time, must reside within the flat part of the high-voltage acceleration waveform. At the ends of the beam bunch, the significant longitudinal space charge force must be balanced by an approximately triangular “ear” waveform with a rise time similar to that of the beam pulse [Sh96]. This resembles the barrier bucket pulses employed, for example, in the KEK Digital Accelerator [Ta12].

For HIF, thyatron or spark gap switched lumped element pulse forming networks, or distributed pulse-forming lines, might meet the pulser requirements except for the required lifetime. However, for the HIDIX (or IRE) research facility previously mentioned, designed for HIF target physics and demonstrating many aspects of accelerator and beam physics at full or relevant scale, continuous 5-15 Hz operation for a year is not required to accomplish the goals. Thus, the lifetime of spark gap switches or thyatrons could be adequate for years of HIDIX operation.

For the low energy end of the HIF accelerator (characterized by a bunch length $> 1 \mu\text{s}$), recent R&D on insulated-gate bipolar transistor (IGBT) switched modulators for the Next Linear Collider (NLC) klystrons and magnetrons appears promising [Ca01]. Each IGBT switches 800 A at 3 kV, and with many IGBT switches in a series and parallel array, a voltage pulse of 400 kV and 2 kA can be generated. IGBTs can switch at a higher power than metal oxide field-effect transistors (MOSFET), but are too slow for the $\sim 0.2 \mu\text{s}$ pulses characteristic of most of the accelerator. However, by using solid-state switches in conjunction with magnetic pulse compression, the rise time requirements might be met [Ta11]. There has been relevant progress aimed at developing high-voltage and high-current pulses for the Elektra IFE laser project [He10]. It remains to be seen if the waveform flatness for HIF ($< 1\%$) can be achieved in a magnetic pulse compression circuit with a sufficiently fast rise time.

At the high energy end of the accelerator, MOSFETs have the needed rise time, but the package size (few kV and 10's of amps) necessitate a much larger array of components to get to the 40 - 100 kV level needed to drive an induction cell. A large MOSFET array (40 x 50) capable of > 10 MW switching [Ba95] was tested for HIF. In tests with the MOSFET array driving a full size Astron induction core and a simulated resistive beam load, > 50% efficiency was achieved. These electronically controlled output pulsers can produce the desired waveforms but have not been widely used because of their high cost.

In summary, switches are integral parts of the pulser, and solid-state switches would have the needed lifetime for a HIF power plant. The remaining challenges are to develop a pulser with the rise time needed for most of the accelerator. Research for other applications (eg: NLC, laser IFE) is relevant, but a dedicated research program for HIF would be an essential component of a balanced R&D portfolio.

2.2 Magnetic materials

A low loss magnetic material with a large flux swing is desired for the induction cores. Ferrites have a modest flux swing, as characterized by the saturation flux ($2B_s > 0.7 - 1.2$ T). Due to their high resistivity, ferrites have been frequently used in induction accelerators with pulses less than $\approx 0.1 \mu\text{s}$.

However, more volt-seconds (Eq. 1) are required for the HIF induction driver. The development of amorphous metallic glass beginning in the 1970's was driven by the energy saving potential for the 50 - 60 Hz electric power industry. The maximum flux swing of amorphous metallic glass lies in the range 2.1 - 3.3 Tesla. The useable flux swing is less than the maximum, because of the difficulty of driving the magnetic material far into saturation. Since the resistivity is much lower than ferrites, the cores are wound with thin, insulated laminations. The flexible 15 - 40 μm tape, with a low magnetization current, was developed first by Allied Signal with the trade name Metglas[®]. Variants have been developed by others, for example, Finemet[®], a nanocrystalline material by Hitachi. The the higher flux swing from annealing is compromised if the material is mechanically manipulated after annealing, thus there has been considerable effort toward annealing in place, or developing winding techniques

that handle the material with low stress to preserve the higher flux swing available and lower loss. Annealing temperatures are in the range 400°C.

For the HIF application, the core is driven at high magnetization rates ($dB/dt \approx 10 \text{ T}/\mu\text{s}$) and the voltage drop between laminations can be tens of volts depending on the width of the material. The surface resistance due to naturally occurring oxidation does not provide sufficient voltage insulation between the individual layers and additional insulation is required. Due to the importance of the eddy current loss mechanism at high magnetization rates, and the need for additional insulation between layers, several types of ferromagnetic wound cores were tested by for the HIF application [Mo02]. Various methods for including insulation in the winding process, preferably compatible with the annealing have also been studied.

Assuming a flux swing of 2.6 Tesla, the amount of required core material for HIF is still significant: To illustrate, assume a pulse length of 250 ns for most of the accelerator ($dB/dt \approx 10.4 \text{ T}/\mu\text{s}$), with a radial build of 0.75 m outside a 1.5 m diameter cluster of beams. 5 GeV of acceleration requires approximately $3 \times 10^7 \text{ kg}$ of ferromagnetic material. A decrease in cost of wound cores is desirable, presently around \$20/kg USD in large quantities. Estimates by industrial manufacturers of projected costs for HIF power plants have been significantly lower.

3 Application to heavy ion fusion

A driver would have a few thousand acceleration stations (or gaps) and focusing arrays, so the required reliability of individual components is high. However, in contrast to induction accelerators for high-current electron beams, where $\beta \approx 1$ shortly after injection, the heavy ion beams in a HIF driver have $\beta < 0.3$ at the end of the accelerator. This allows for feed-forward correction of the waveform imperfections: an error on a voltage or beam current waveform could be detected and corrected using dedicated correction modules. In fact, if one pulser or acceleration module misfires, occasionally or repeatedly, a nearby spare module, if incorporated into the accelerator lattice could be triggered to compensate on the same pulse. Relatively small correction cores periodically placed in the accelerator lattice, driven by a pulser that can actively regulate the output

voltage (eg. MOSFET controlled), could correct voltage errors on the order of 1%. The detection of small amplitude errors is limited by signal-to-noise in the pulsed power environment. Uncorrelated errors in successive pulsers will accumulate, with the summed amplitude proportional to the square root of the number of modules under consideration. This has led to an estimated random voltage tolerance of 1% per module on the flat top of the waveform. The systematic errors, for example from a non-ideal PFN, will be repeated in each successive pulser. This might cause a droop on the flattop of the pulse, and must be corrected more frequently. The research at KEK [Ta12] on the induction synchrotron is developing capability that is relevant to high-precision corrector cores and pulsers for a HIF induction linac.

3.1 Transverse focusing

There are two main types of focusing magnets for a driver: focusing quadrupoles in the accelerator and final focusing magnets near the target chamber. For beam physics, engineering and economic reasons they are superconducting. Dipoles or displaced quadrupoles for bending are a relatively minor component of the driver.

Perhaps the most unusual characteristic of the induction accelerator for HIF is the approach to transverse beam focusing by subdividing the charge into many beams and focusing them in a close-packed array of quadrupoles. All the beams thread common induction cores, as illustrated in Figs. 4 and 5, and the goal to transport a large overall current (sum over many beams) to enable high accelerator efficiency is accomplished. This design is motivated by two considerations: In order to meet the focal spot required at the fusion target, the ~1 mC of charge cannot plausibly be focused in a single beam due to high space charge and emittance, which is remedied by subdividing the charge into separate beam bunches, which overlap only at the target.

Subdivision also leads to a compact induction core: In the accelerator, many such beams with low emittance in a suitably designed array may be transported more compactly through the induction cores than a single higher current beam. The transportable beam current is given by:

$$I_{max} \approx 4 \times 10^{-12} a B v^2 \quad (\text{Eq. 2})$$

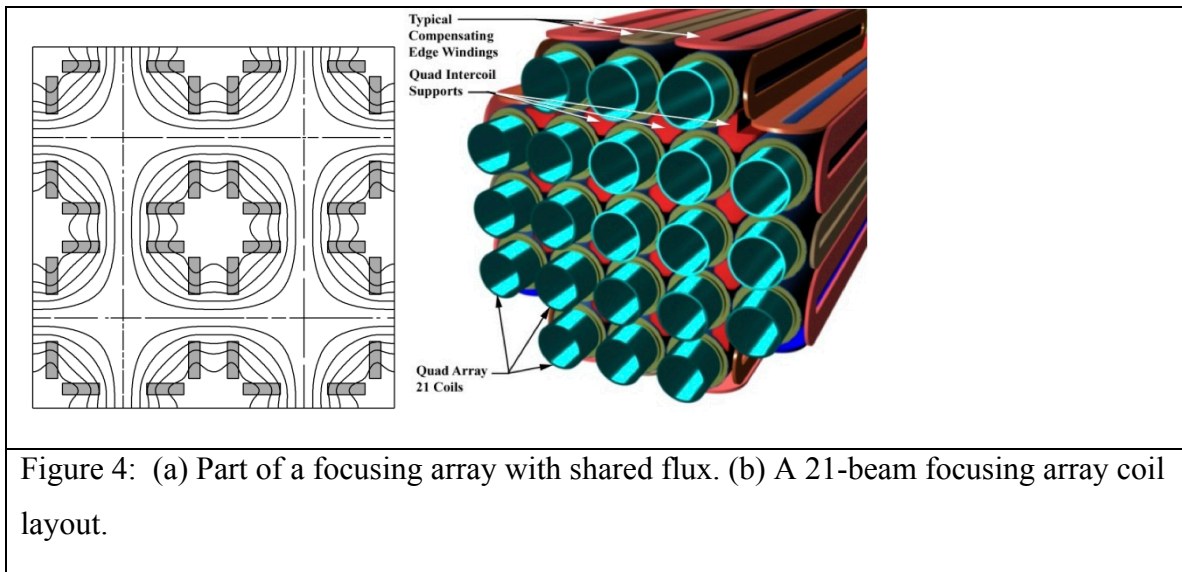
in mks units, where a is the beam aperture radius, B is the pole tip field, and v is the ion velocity. For electrostatic quadrupoles, $B \rightarrow E/v$, where E is the electric field. Each beam in the accelerator is space charge dominated, that is, the transverse envelope of the beam is determined mostly by the space charge being balanced by the applied focusing field. The longitudinal and transverse beam dynamics are summarized in these proceedings [Le12].

The repeat structure in the accelerator is the half-period L , which has a quadrupole of length ηL , and an accelerating column of length $(1-\eta)L$. The quadrupole occupancy factor, η , varies from about 0.8 at the beginning of the accelerator to about 0.1 at the end, with most of the machine having the lower occupancies.

For an occupancy η , well above 0.5, there is insufficient space for induction cores separated axially from the focusing quadrupoles. Thus, at the low energy end of the driver, the focusing quadrupoles are located within the axial extent of the cores, while at higher energy, where $L > 2$ m, the occupancy is smaller, and the drift space between adjacent quadrupoles is much greater, the quadrupoles are located between the induction cores. This simplifies manufacturing, installation, and maintenance of the quadrupole arrays and the acceleration modules for most of the accelerator. Electrostatic quadrupoles at low energy have the attractive feature of compactness and their natural clearing of stray electrons (electron clouds) that would perturb the space charge distribution and adversely affect the beam emittance. Arrays of magnetic quadrupoles, more effective at higher ion velocity (Eq. 1) tend to optimize for higher current or line charge density than electrostatic quadrupoles. Merging groups of four beams from the electrostatic array into single beams at the transition to the magnetic array has been considered and explored in a series of experiments and particle simulations [Se03].

A system with magnet lengths of <1 m, peak field in the winding of 4 T, and occupancy $\eta < 0.5$ characterize most of the accelerator. Average losses of ~ 1 Watt/lattice period in the magnet leads of each array module, and 1 W/m^2 within the superconducting magnets beam tubes result in a relatively low power required of the refrigeration system. A schematic of the packing of quadrupoles and beams is shown in Fig. 4. The flux is

shared among adjacent quadrupoles, and thus enhances the field in the aperture of the neighbors by approximately 30%.



The number of beams typically lies in the range 48-120. The design of a prototype array is shown in Fig. 4(b). At the periphery of the array, the coil and magnetic boundary condition must satisfy the field quality requirements of the outside beams. Furthermore, if the induction core is nearby, the return flux is designed to not enter the ferromagnetic material, in which the permeability is varying during the acceleration pulse as the core approaches saturation. A solution to the termination of the field at the edge of the focusing array is described in Ref. [Fa99]. In addition, centroid correction (steering) dipoles must be implemented with a frequency sufficient to maintain satisfactory beam quality and particle loss.

3.2 Proposed near term research

Though many components of the accelerator architecture have examples in existing accelerators, an induction linear accelerator on the scale of a 10-100 kJ research facility (eg: HIDIX) would be unprecedented. To reduce the risk for such a facility, accelerator research and development is suggested below.

An ongoing question for 5-10 Hz operation of the accelerator is whether the pressure inside the beam lines, which is expected to rise immediately after a beam pulse, can be lowered fast enough for the next pulse or even be damaging to the same pulse. The source of the pressure rise is particle loss to the structure wall, which in turn desorbs a

large number of neutral atoms or molecules. A 5 - 10 Hz experiment aimed at quantifying and developing techniques to control the pressure rise, at least at the presently attainable beam energy (up to 2 MeV) and intensity, could be performed with minor modifications to existing equipment.

There will be a need to address driver beam physics questions summarized by Lee [Le12]. Topics of interest include transverse emittance growth of high space-charge beams caused by envelope mismatch, non-linear space charge distributions, beam centroid control, imperfect applied fields, electron clouds and beam-gas interactions and the possible interactions between multiple high-current beams [Fr01]. Collective effects of space charge waves are expected to relax after several plasma oscillations, corresponding to 40 - 100 quadrupoles (lattice half periods). Many issues may be addressed with a single beam accelerator, thereby reducing the cost of this research compared to a many-beam accelerator of equal length. Halo formation and control via periodic collimation would also be explored. Cohen [Co12] has also summarized the mechanisms for beam quality degradation due to electron clouds, which would also be explored in the same experimental facility.

A multiple beam experiment demonstrated simultaneous acceleration and focusing of four heavy ion beams in an induction linac [Fa96]. The beam current was low, so that beam-beam and beam-core interactions were negligible. The experimental exploration of these effects requires much higher beam current (> 100 A) such as envisioned for the HIDIX. We note that multiple, high-current electron beams in an induction linac have also been demonstrated [Pr83, Ha85].

HIF system studies show cost reductions for high gradients (2-4 MV/m) but data for such extrapolations are scarce. The acceleration gap designs usually include several plates electrically connected to the column for grading, with multiple apertures through which the numerous beams pass, as shown in Fig. 5. These plates partially isolate the high space charge beams from each other. Stray particles (ions or electrons) striking the insulator are potential seeds of HV breakdown, so, as in electron induction accelerators, the columns may need shielding structures to block the charged particles from striking the insulators along with grading electrodes to achieve the highest gradient. In the

systems studies, the gradient has been sometimes limited to about 1 MV/meter. The basis for this limit has been the < 1 MV/meter gradient in electron beam induction linacs, and also the scarcity of relevant experimental data on column HV holding above ≈ 1 MV. Electron induction accelerators approached 1 MV/m, with little data for ion accelerators at or beyond that gradient. Some approaches that might lead to increased gradient for HIF drivers include the implementation of radial insulators (vs. insulating columns entirely parallel to the beamline), and the utilization of high-gradient insulators based upon very thin layers of graded columns [Ca09]. A test stand in an induction voltage adder configuration [Sm04] capable of measuring the voltage holding limits at full scale (1 - 4 MV/m) would enable more confident designs and cost estimates for a HIDIX and a driver.

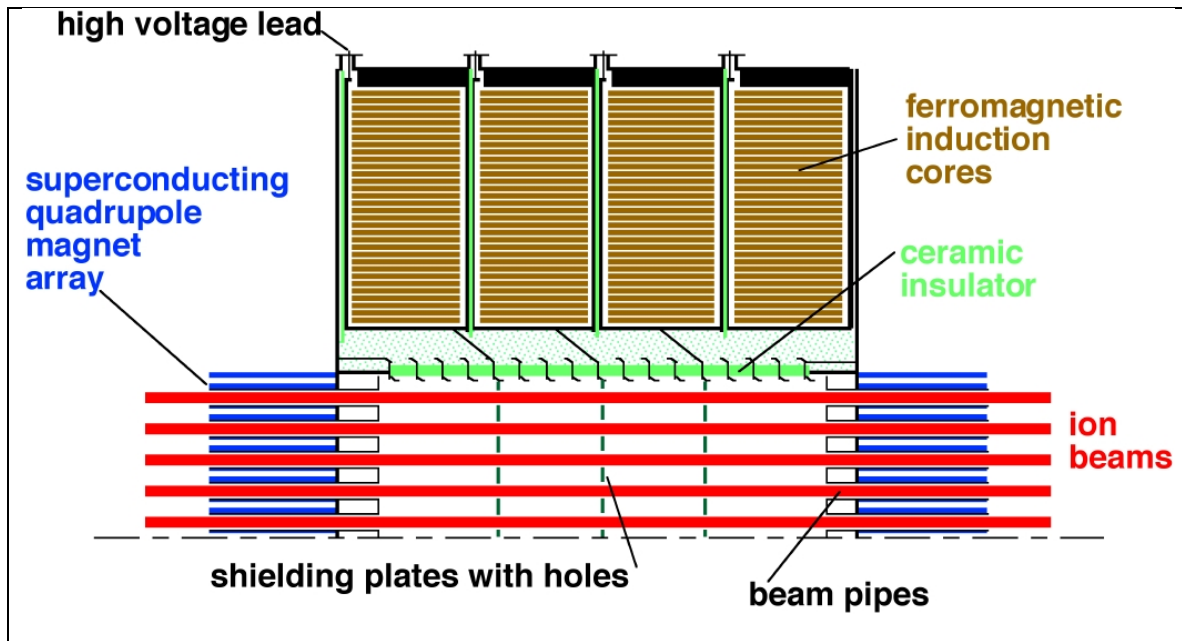


Figure 5: Cross section view of a multiple beam induction acceleration and focusing module for heavy ion fusion.

In the area of pulsers for the induction modules, solutions for a HIDIX are available, because switch lifetime is not as demanding as in a power plant. However, the development of solid state switched pulse-forming networks or lines with the required driver lifetime are still needed. Amorphous ferromagnetic tape is the best induction core

material so far, but methods for providing adequate insulation between the layers of tape and realizing the greater flux swing of annealed material requires further research.

The issues of superconducting magnetic quadrupole arrays for many parallel channels can be addressed using a restricted number of channels, as long as proper transverse termination of the fields is provided. Thus, a critical next step would be a prototype array with only four or nine channels. This would follow on the results of past successful prototype magnet designs; single quadrupoles derived from the array concept. The R&D ended in 2004 with the production and successful testing of a prototype quadrupole doublet in a compact cryostat suitable for transport and acceleration of intense beams of ($\lambda \approx 0.2 \mu\text{C/m}$) K^+ through ~ 100 quadrupoles, or several beam-plasma oscillations [Gu05].

Together with complementary research on fusion target physics, ion sources and injectors, and beam compression and final focusing, the above research would be necessary to reduce the risk and develop a credible basis for a HIDIX accelerator design. Even with a relatively small budget, there are R&D opportunities to make significant progress aimed at heavy ion inertial fusion.

4 Acknowledgements

This work was supported by the U.S. Department of Energy under contract numbers DE-AC02-05CH1123 and DE-AC52-07NA27344.

References

- [Kw05] J.W. Kwan, *High Current ion sources and Injectors for Induction Linacs in Heavy Ion Fusion*, IEEE Trans. On Plas. Sci., 33 (2005) 1901
<http://ieeexplore.ieee.org/stamp/stamp.jsp?arnumber=01556676>
- [Ka12] I. Kaganovich et al., *Drift Compression and Final Focus*, these proceedings.
- [Ol12] C. Olson, *Chamber Transport for Heavy Ion Fusion*, these proceedings.
- [Mo12] R. Moir, *Liquid Wall Chambers for HIF*, these proceedings.
- [Ba12] R.O. Bangerter, *Heavy Ion Targets*, these proceedings.

426 [Le12] E.P. Lee, *Beam Dynamics for Induction Accelerators*, these proceedings.

427 [Fr12] A. Friedman, *Differential acceleration in the final beam lines of a Heavy Ion*

428 *Fusion driver*, these proceedings.

429 [Yu03] S. S. Yu, et al., *An Updated Point Design For Heavy Ion Fusion*, Fusion Sci.

430 Technol. 44, 266 (2003) <http://escholarship.org/uc/item/6vq5x9x8>

431 [Na13] *An Assessment of the Prospects for Inertial Fusion Energy*, National Research

432 Council. Washington, DC. The National Academies Press, 2013. ISBN 978-0-309-

433 27081-6 http://www.nap.edu/openbook.php?record_id=18289

434 [Ti85] M. G. Tiefenback and D. Keefe, *IEEE Trans. Nucl. Sci.* **NS-32**, 2483 (1985); T. J.

435 Fessenden, *Nucl. Instr. Meth. Phys. Res. A* **278**, 13 (1989).

436 [Bi05] F. M. Bieniosek, et al., *2-MV electrostatic quadrupole injector for heavy-ion*

437 *fusion*, PRST-AB 8, 010101 (2005). <http://prst-ab.aps.org/abstract/PRSTAB/v8/i1/e010101>

438 [Pr05] L.R. Prost, et al., *High current transport experiment for heavy ion inertial fusion*

439 <http://link.aps.org/doi/10.1103/PhysRevSTAB.8.020101>

440 [Sh11] W. M. Sharp et al., *Inertial Fusion Driven By Intense Heavy-Ion Beams*, Proc.

441 Part. Accel. Conf. 2011, New York, NY, USA

442 <http://accelconf.web.cern.ch/AccelConf/PAC2011/papers/weoas1.pdf>

443 [Go79] T. Godlove, *Recent Progress and plans for Heavy Ion Fusion*, Proc. Part. Accel.

444 Conf., IEEE Transactions on Nuclear Science Vol. NS-26, No. 3, June 1979

445 http://accelconf.web.cern.ch/accelconf/p79/PDF/PAC1979_2997.PDF

446 [Ba01] J.J. Barnard et al., *Planning for an Integrated Research Experiment*, Nuclear

447 Instruments and Methods in Physics Research A 464 (2001) 621–628

448 <http://escholarship.org/uc/item/7r43j8sp>

449 [Lo11] B.G. Logan, *Ion-Beam-Driven Inertial Fusion Energy*, Presented at the Second

450 Meeting of the National Academies of Sciences and Engineering, January 29, 2011–

451 *Prospects for Inertial Confinement Fusion Energy Systems*, National Academies Review,

452 http://fire.pppl.gov/IFE_NAS2_HIF_Logan.pdf

453 [Ch58] N. Christofilos. *Astron thermonuclear reactor*, In 2nd UN International

454 Conference on Peaceful Uses of Atomic Energy, Vol. 32, page 279, Geneva, Switzerland,

455 1958; N. Christofilos. *Energy Balance in the Astron Device*, Nucl. Fusion Suppl. I, page
 456 159, 1962.

457 [Ta11] K. Takayama, R.J. Briggs, editors, *Induction Accelerators*, Springer –Verlag
 458 (2011) DOI 10.1007/978-3-642-13917-8.

459 [Sh96] W. M. Sharp, *et al.*, *Effects of Longitudinal Space Charge in Beams for Heavy-*
 460 *Ion Fusion*, Fusion Eng. Design **32-33**, 201 (1996)
 461 <http://www.osti.gov/bridge/servlets/purl/192508-UbT7Xj/webviewable/192508.pdf> .

462 [Ta12] K. Takayama, et al., *KEK Digital Accelerator and Latest Switching Device R&D*,
 463 These proceedings.

464 [Ca01] R.L. Cassel et al., *The Prototype Solid State Induction Modulator For SLAC NLC*,
 465 Proc. PAC 2001, <http://accelconf.web.cern.ch/AccelConf/p01/PAPERS/FPAH033.PDF> ; *NLC*
 466 *Hybrid Solid State Induction Modulator*, Proc. Linac 2004,
 467 <http://accelconf.web.cern.ch/AccelConf/I04/PAPERS/THP42.PDF> ; R.L. Cassel et al., *An all Solid*
 468 *State Pulsed Marx Type Modulator for Magnetrons and Klystrons*, Pulsed Power
 469 Conference, 2005 IEEE , vol., no., pp.836-838, 13-17 June 2005
 470 DOI:10.1109/PPC.2005.300791
 471 <http://ieeexplore.ieee.org/stamp/stamp.jsp?tp=&arnumber=4084347&isnumber=4084141>

472 [He10] F. Hegeler, M.W. McGeoch, J.D. Sethian, H.D. Sanders, S.C. Glidden, M.C.
 473 Myers, M.F. Wolford, *A durable, repetitively pulsed, 200 kV, 4.5 kA, 300 ns solid state*
 474 *pulsed power system*, Power Modulator and High Voltage Conference (IPMHVC), 23-27
 475 May 2010, doi:10.1109/IPMHVC.2010.5958284
 476 <http://ieeexplore.ieee.org/stamp/stamp.jsp?tp=&arnumber=5958284&isnumber=5958279>; J.D. Sethian
 477 et al., *ELECTRA: A Repetitively Pulsed, Electron Beam Pumped Krf Laser To Develop*
 478 *The Technologies For Fusion Energy*, 2005 IEEE Pulsed Power Conference
 479 <http://dx.doi.org/10.1109/PPC.2005.300463>

480 [Ba95] W.A. Barletta, A. Faltens, E. Henestroza, E. Lee, *High current induction linacs*,
 481 1995 AIP Conf. Proc., <http://link.aip.org/link/doi/10.1063/1.49154>

482 [Mo02] A.W. Molvik, A. Faltens, *Induction core alloys for heavy-ion inertial fusion-*
 483 *energy accelerators*, PRST-AB 5, 080401 (2002)
 484 <http://link.aps.org/doi/10.1103/PhysRevSTAB.5.080401>

485 [Se03] P.A. Seidl et al, *Scaled beam merging experiment for heavy ion inertial fusion*,
 486 PRST-AB 6, 090101 (2003) <http://link.aps.org/doi/10.1103/PhysRevSTAB.6.090101>

487 [Fa99] A. Faltens, D. Shuman, *A superconducting quadrupole array for transport of*
 488 *multiple high current beams*, Proc. 18th IEEE/NPSS Symposium on Fusion Engineering.
 489 IEEE Symposium Proceedings 99CH37050, pp. 362-6 (1999)
 490 <http://ieeexplore.ieee.org/stamp/stamp.jsp?arnumber=00849857>

491 [Co12] R. Cohen, *Electron clouds in HIF drivers*, these proceedings.

492 [Fa97] W. M. Fawley, et al., *Beam dynamics studies with the heavy-ion linear induction*
 493 *accelerator MBE-4*, Phys. Plasmas 4 (1997) 880.
 494 http://pop.aip.org/resource/1/phpaen/v4/i3/p880_s1

495 [Pr83] K. R. Prestwich, et al., IEEE Trans Nuc. Sci. 30, 1983, p.3155

496 [Ha85] D. E. Hasti, et al., IEEE Pulsed Power Conf., 1985, p. 35

497 [Fr01] A. Friedman et al., *Beam simulations for IRE and driver: status and strategy*,
 498 Nuc. Inst. and Methods A 464 (2001) 653–661.

499 [Ca09] George J. Caporaso et al., *Status of The Dielectric Wall Accelerator*, Proc,
 500 PAC09, <http://accelconf.web.cern.ch/AccelConf/PAC2009/papers/th3gai02.pdf>

501 [Gu05] Chen-yu Gung, et al., *Construction and Tests of HCX Quadrupole Doublet for*
 502 *Heavy Ion Beam Transport Experiments*, IEEE Trans. Applied Superconductivity, 15,
 503 NO. 2, (2005) <http://dx.doi.org/10.1109/TASC.2005.849523>

504 [Sm04] I.D. Smith, *Induction voltage adders and the induction accelerator family*,
 505 PRST-AB 7, 064801 (2004) DOI: 10.1103/PhysRevSTAB.7.064801